Theor. Appl. Climatol. 63, 129–139 (1999)

Theoretical and Applied Climatology

Institute for Atmospheric Physics, GKSS-Forschungszentrum, Geesthacht, Germany

Wind Climate Simulation over Complex Terrain and Wind Turbine Energy Output Estimation

H.-T. Mengelkamp

With 9 Figures

Received November 13, 1998

Summary

A statistical-dynamical downscaling procedure is applied to investigate the climatological wind field over a complex terrain area in central Germany. The model domain, 80×87 km, is dominated by flat terrain in the westerly and northerly part and encompasses the Teuteburger Wald and the Wiehengebirge areas with hills up to 330 m a.m.s.l. in the southeasterly region. The downscaling procedure combines a large-scale regionally representative wind statistic and a high-resolution numerical atmospheric mesoscale model. A cluster analysis of a 12-years time series of radiosonde data provides 143 clusters each being a combination of the geostrophic wind components and the vertical temperature gradient. These parameter sets constitute the reference state for highly-resolved steady-state wind field simulations with a non-hydrostatic model. Weighting the resulting wind fields with the corresponding cluster frequency gives climatologically representative frequency distributions of the wind speed and -direction.

A comparison of observations at synoptic stations with simulation results shows a good agreement regarding the mean wind speed but larger differences for low wind speeds and an over-representation of southwesterly wind directions.

By combining the wind speed frequency distribution with the power curve of wind turbines the yearly energy output of 46 wind turbines inside the simulation domain was calculated and compared to the actual production. No bias or systematic trend in the deviation was found. The relative differences for the smallest turbines reach 100 percent with a decreasing tendency to larger units.

1. Introduction

The growing interest in renewable energy resources during the last decade has led to the establishment of a wind energy industry in Europe and resulted in a rapidly increasing number of installed wind turbines. The design, planning and operational aspects of wind energy systems require detailed knowledge of the wind field characteristics. We focus on the planning aspect, i.e. the wind resource estimation which ranges from a regional assessment of the available energy in the wind on a large scale to the calculation of wind speed statistics at particular wind turbine sites. Such studies are often based on long-term wind records from near-surface measurements at synoptic stations. The models available for wind turbine siting exhibit a wide range of complexity ranging from mass-consistent models to non-hydrostatic mesoscale models.

Troen and Petersen (1989) used a two-dimensional, two-layer boundary layer model to develop the European Wind Atlas and Analysis System WASP. This model chain corrects near-surface wind measurements for orographic, roughness and obstacle induced effects and calculates the wind climate at any particular site. Due to the simple turbulence parameterization and the linearization of the equations of motion the application of this model is restricted to flat or gently sloping terrain. A series of mass consistent models has also been developed to compute the wind field over complex terrain (Bhumralkar et al., 1980; Guo et al., 1990;

Sherman, 1978; Endlich et al., 1982). These models assume mass continuity and minimize the difference between the computed and the observed wind fields, with the latter being deduced by extrapolation and interpolation of surface measurements. The resulting wind field, however, depends much on the quality of the observed wind field (Guo et al., 1990; Groß, 1996) and in mountainous terrain in particular it is necessary that the observations already approximately represent the wind characteristics over the area under investigation (Endlich et al., 1982).

Over complex and heterogeneous terrain near-surface measurements are often influenced by local, dynamically or thermally induced circulations, and by close obstacles or vegetation which cannot adequately be corrected for (Wieringa, 1983). In addition, the spatial density of wind observation sites is usually inadequate to deduce high-resolution wind speed maps from measurements alone. To overcome these shortcomings statistical-dynamical downscaling approaches have been applied which combine a statistical or synoptic classification of the climatological regime and a high-resolution numerical model. Wipperman and Groß (1981) reproduced orographically influenced wind roses by downscaling the geostrophic wind speed distribution using a two-dimensional version of a mesoscale model. Segal et al. (1982) studied the wind energy characteristics over central Israel by use of a two-dimensional version of a hydrostatic mesoscale model. Because the wind field was mainly thermally forced only three synoptic classes were chosen (one day in summer and one day in winter and an advective Sharov situation) for which full daily cycles were simulated. Bergström (1996) studied the wind field over the Baltic Sea area with a hydrostatic model and classified the overall climatology into four seasons (January, April, July and October), three wind speed classes (5, 10 and 15 m/s), eight wind direction sectors and three mean surface temperatures over land. The climatological wind field was derived by weighting 288 runs.

In a similar study Sandström (1997) ignored the variation in surface temperature and concluded that 96 model runs did cover the most important conditions that determine the boundary layer wind field. The difference between modeled and observed mean wind speeds at the location of two lighthouses ranged from 0.1 to 0.5 m/s. Comparisons with ship measurements showed differences of less than 0.5 m/s over the main part of the Baltic Sea. Heimann (1986) calculated the annual frequency distribution of surface winds over the Main-Taunus region with a three-layer hydrostatic model. Cycles of typical days for each of twelve wind direction sectors were simulated using an annual mean value for the geostrophic wind speed. This approach was extended by Frey-Buness et al. (1995) to the regionalization of climate change scenarios by classifying large-scale synoptic situations derived from multi-year episodes of global climate simulations. In order to include a classification criterion with emphasis on precipitation they selected a winter and a summer situation for twelve wind direction classes, respectively. They also distinguished further 'fair weather' and 'poor weather' situations which were classified with respect to cloudiness. In a different method to all other complex-terrain studies which use upper air data, Brücher et al. (1994) calculated the frequency of occurrence of the basic state classes from near surface observations by an inversion technique. Choosing 60 classes for the basic state defined by wind speed, direction and stratification they simulated the spatial distribution or orographically influenced wind roses.

The selection of appropriate parameters and their classification to define the climatological regime is as essential for any dynamic downscaling procedure as the choice of the numerical model and the mode of simulations. While all the previously mentioned studies used a fixed classification scheme here we apply a cluster analysis to group the reference states which are defined by geostrophic wind speed components and static stability. The advantage of this methodology is outlined in section 2. Use of a non-hydrostatic mesoscale model provides a spatial resolution high enough to compare model results with point observations even over complex terrain. The model and the simulation area are described in section 3. Section 4 comprises the climatological wind field and its comparison with observations. The relationship of this study to wind energy applications is then stressed in section 5.

2. The Statistical-Dynamical Downscaling Approach

Straight forward methodologies for deriving a highly resolved climatological wind field over complex terrain need to be a very dense network of good quality measuring stations operating over a long enough time period (e.g., more than 10 years for our purposes) or this can be achieved through the improvement of the spatial resolution of climate models and long-term simulations. However, as these approaches are not feasible here, we rely on so-called downscaling methods which link large scale coarse-grid information with regional and small-scale processes. Out of the strategies discussed by Giorgi and Mearns (1991) and Storch (1995) the statistical-dynamical downscaling approach seems to be the most appropriate methodology for wind climate simulations as it does not require any calibration with observed data (like the statistical method) or large computational demands as required for long-term high-resolution simulations with a limited-area model forced with time-dependent boundary conditions from a climate model (like the nesting approach). Components of the statistical dynamical downscaling approach (Fig. 1) are

- a time series of an appropriate parameter set which is representative for a larger area
- a classification scheme which groups the large amount of data into defined categories
- a numerical model which performs simulations for each of these categories
- a postprocessing program which sums and weights the particular simulation results

The statistical-dynamical downscaling methodology is based on the assumption that the climate for a given region can be described by a classification of an appropriate set of atmospheric parameters which characterize typical flow patterns ("Großwetterlagen"). For wind climate simulations over inland complex terrain the important parameters are

- the geostrophic wind speed and direction
- the thermal stratification in the atmospheric boundary layer
- the orography
- the surface roughness

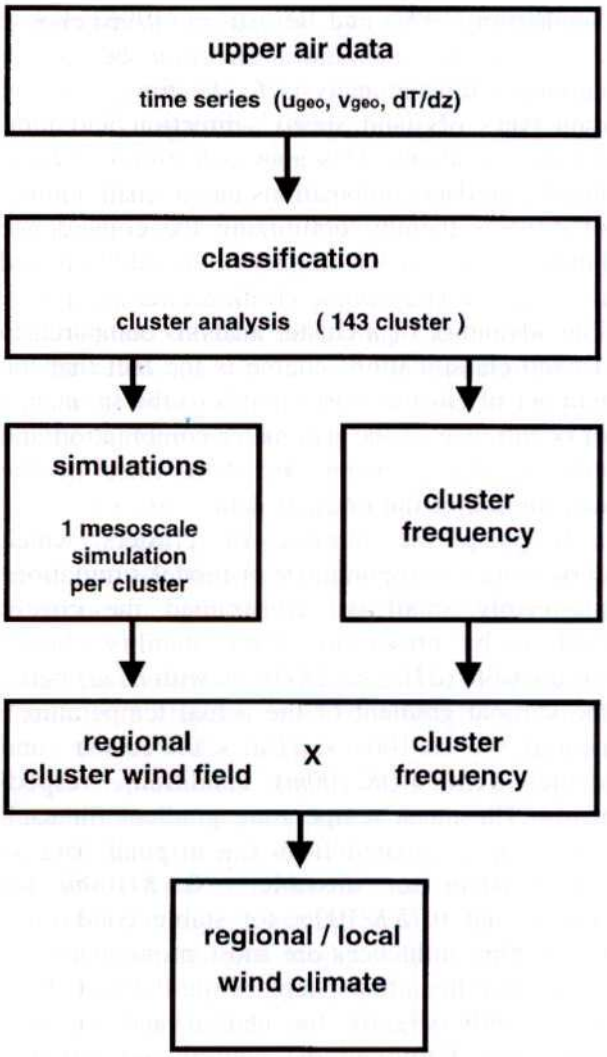

Fig. 1. Flow chart of the statistical-dynamical downscaling approach

The atmospheric data were taken from a 12-year time series (1979–1991) of 12-hourly radiosonde ascents at the weather station Hannover which is located roughly 100 km distant from our modelling area. Wind speed and direction were measured at 850 hPa and the vertical temperature gradient between 100 m and 1.5 km height. The orography was available on a 50 m grid and distance weighted onto a 1×1 km grid. Surface roughness was digitized from topographic maps.

As this study aims to provide information about wind power density which depends non-linearly on wind speed, the classification of the forcing parameter is most important. Different to other studies which have used a fixed classification scheme for the geostrophic wind (e.g.,

Sandström (1997) and Bergström (1996) choose 3 wind speed values and 8 direction sectors) we applied a cluster analysis to the time series of data pairs of wind speed, -direction and temperature gradient. This approach groups a large number of data combinations into a small number of clusters thereby optimizing the coincidence between the cluster frequency distribution and the original data sample (Kalkstein et al., 1987). The advantage of a cluster analysis compared to a fixed classification scheme is the fact that the number of clusters corresponds to the frequency of occurrence of the parameter combination and that the cluster means are determined by the distribution of the original data.

To keep the number of clusters which corresponds to the number of model simulations reasonably small we constrained the cluster analysis by prescribing three stability classes for unstable ($dT/dz < -1K/100m$ with dT/dz being the vertical gradient of the actual temperature), neutral ($-1K/100m < dT/dz < 0K/100m$) and stable ($dT/dz > 0K/100m$) conditions, respectively. The mean temperature gradient for each class was calculated from the original data as $-1.2\,K/100m$ for unstable, $-0.6\,K/100m$ for neutral and $0.75\,K/100m$ for stable conditions. Orographic influences are most pronounced for stably stratified atmospheres while the wind field differs only slightly for neutral and unstable conditions. Grouping the neutral and unstable conditions together could have been justified and would have lowered the total number of cluster simulations. This argument is followed by Brücher et al. (1994), however, because of the high sensitivity of wind power to wind speed variations we kept three stability classes. We also limited the total number of clusters not only because of limited computer resources but also because we aimed at producing a similar standard deviation for wind speed and -direction in each cluster. A total of 143 clusters was found to appropriately represent the original time series. Figures 2 and 3 show that the frequency distributions of wind speed and -direction of the cluster data coincide fairly well with the original data.

Each cluster represents a particular set of the geostrophic wind speed and the temperature gradient. These two parameters define the large-scale situation as the basic state for the

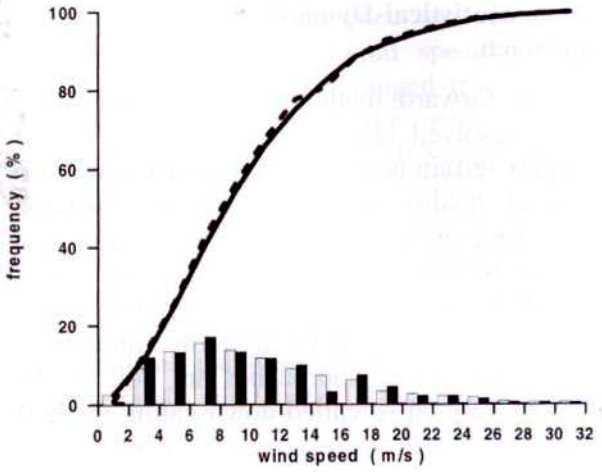

Fig. 2. Cumulative and relative frequency distribution of wind speed of the original data (solid line and grey bars) and the cluster data (dashed line and black bars)

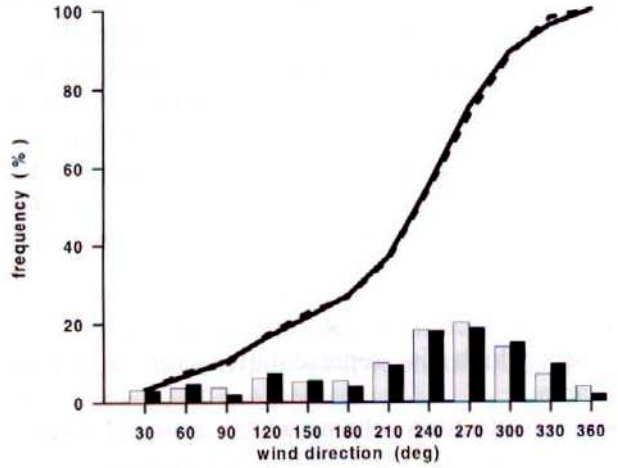

Fig. 3. Cumulative and relative frequency distribution of wind direction of the original data (solid line and grey bars) and the cluster data (dashed line and black bars)

regional model simulations. The simulations determine the influence of small-scale topographic features (orography and roughness) on the basic atmospheric state which is assumed to inherently reflect synoptic-scale patterns such as low pressure systems travelling over the area of interest. For each of these clusters a steady-state simulation with the non-hydrostatic mesoscale model GESIMA (Geesthacht Simulation Model of the Atmosphere) is performed. When using the prognostic model in a dynamic mode we assume that thermal effects are either accounted for through the vertical temperature gradient or

of minor importance for a wind energy survey, because of their dominant occurrence during low wind speed conditions. Over the inland hilly terrain of central Germany the most significant mesoscale forcing on the wind field is the dynamical effect of topographic structures.

The wind fields of all 143 simulations were weighted with the corresponding cluster frequency giving the average three-dimensional wind field and the frequency distributions of wind speed and -direction at each grid point of the simulation domain.

3. Model Description and the Simulation Domain

3.1 Model Characteristics and Simulation Performance

The numerical model employed for this study is the three-dimensional non-hydrostatic mesoscale model GESIMA. A derivation of the dynamical equations is given in Kapitza and Eppel (1992), parameterizations and test cases are described in Eppel et al. (1995) and Mengelkamp (1991). The system of equations used in GESIMA is based on the conservation laws for momentum, energy, and mass. The dynamical part consists of the anelastic, Boussinesq approximated equations of motion and the continuity equation. The inner energy is represented by a prognostic equation for potential temperature. A first-order closure according to level 2.5 in the hierarchy of Mellor and Yamada (1974) is applied for the turbulent momentum fluxes. The vertical component of the turbulent diffusion coefficient is a function of turbulent kinetic energy for which a prognostic equation is solved neglecting the production of turbulent kinetic energy by horizontal shear (Bougeault and Lacarre, 1989). The equations are formulated in a terrain-following coordinate system and solved by a MacCormack-scheme which is second order accurate in space and time (Anderson et al., 1984).

Detailed parameterization schemes to describe cloud development, the interaction with radiation and the exchange of momentum, energy and water at the soil-vegetation-atmosphere interface are incorporated in the model. However, they are not activated for this study because we are only interested in a climatological wind field which is primarily driven by the synoptic pressure gradient and modified through the orography and surface roughness. We consider diurnal thermal effects as negligible since small-scale thermally driven circulation systems hardly occur over this inland hilly terrain which is characterized by farmland and forests. With the elimination of thermal forcing the prognostic model is used in a so-called dynamic mode which results in a steady-state solution describing the modification of the reference state due to the topography.

The vertical grid spacing increases from 20 m at the surface to 400 m at the upper boundary which is located at 3480 m. The upper 4 layers above 1880 m serve as a damping layer to prevent vertical propagating gravity waves from reflecting. At the lower boundary we prescribed a roughness length for 10 land-use classes ranging from 2 mm for lakes to 2 m for the center of big cities according to Wieringa (1986). Forested areas were characterized by a roughness length of 1 m and a displacement height of 8 m. Any larger displacement height resulted in numerical instabilities being provoked at forested hill tops, due to the terrain-following coordinate system the lowest grid cell was even lower than 20 m. The horizontal grid spacing was set to 1×1 km.

The 3-dimensional model is initialized with a horizontally homogeneous state resulting from a one-dimensional pre-run. The pre-run for each of the 143 clusters was forced by the geostrophic wind speed components at the upper boundary and the vertical temperature gradient from the cluster analysis. A fixed roughness length and surface temperature formed the lower boundary condition. The vertical profiles of wind speed components and temperature were distributed horizontally in the 3-d domain. For variable orography the potential temperature was interpolated to the proper height. The velocities are transformed into mass fluxes through the lateral grid box faces for one reference column. Subsequently, these fluxes are shifted through the domain which automatically satisfies the continuity equation in the 3-d domain (Kapitza and Eppel, 1992). The 3-d steady-state simulations adjust the wind field to the realistic roughness distribution and orography. Wind field convergence was reached after 4 to 6 hours real simulation time depending on the forcing wind speed and stability. The steady-state solution was

assumed to have been reached when the mean of the absolute values of the differences in wind-speed components between two consecutive time steps asymptotically reached a lower limit which varied around a value of the order of 10^{-4} depending on the cluster forcing.

3.2 The Simulation Domain

The model domain (Fig. 4) covers a region of 80×87 km. It is dominated by flat terrain in the westerly and northerly part and encompasses the Teuteburger Wald and the Wiehengebirge turbines with hills up to 330 m a.m.s.l. in the southeasterly region. The hilly regions are almost completely forested (roughness class 8) whereas the flat terrain is characterized by farmland with bushes, smaller groups of trees and small villages (classes 4 and 5). Larger areas of moorland (classes 2 and 3) can be found in the northeastern part of the domain (Fig. 5). The city of Osnabrück can be identified by roughness class 10 at coordinates (3435/5791) (x/y-direction).

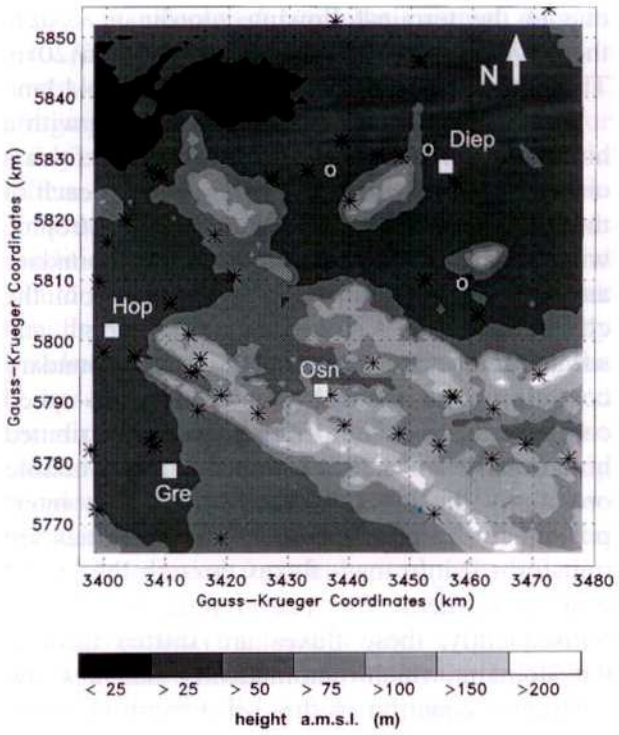

Fig. 4. Orography of the simulation domain. Heights are given in m. The white squares represent locations of synoptic weather stations (the name abbreviations correspond to the cities listed in Table 1), the circles show the WMEP locations and the stars indicate locations of wind turbines

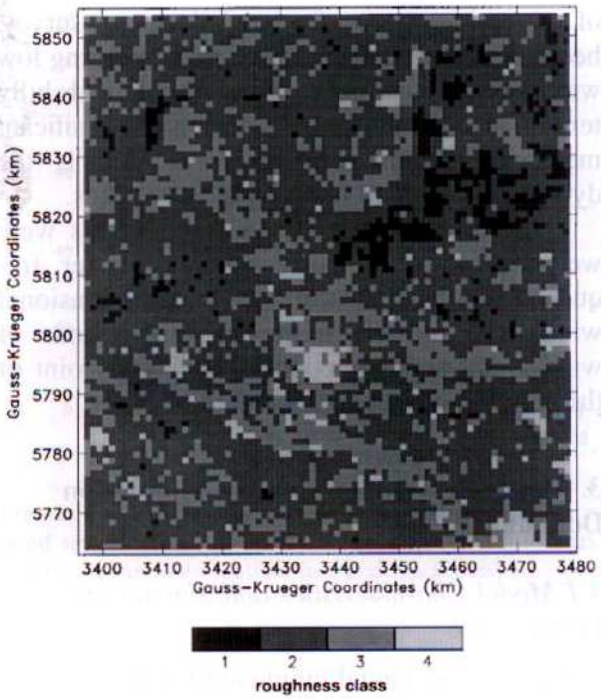

Fig. 5. Roughness characteristic of the simulation domain. The ten roughness classes which form the basis for the simulations are grouped into 4 classes for elucidation purposes. Class 1 includes lakes and open farmland (roughness length 2 mm and 3 cm), class 2 farmland with a closed landscape (roughness length 10, 30 and 50 cm), class 3 comprises forest dominated areas (roughness length 0.5, 0.7 and 1.0 m) and class 4 represents urban areas (roughness length 1.5 and 2.0 m)

4. The Climatological Wind Field

4.1 Wind Speed Distribution

Figure 6 shows the mean wind field at 50 m height calculated by summing the weighted 143 cluster wind fields. With Figs. 4 and 5 in mind it becomes obvious that wind speed values below 5 m/s occur over the forested hilly terrain and the larger cities. Values between 5 and 6.5 m/s can be found over flat and smooth terrain, with the highest values over moorland areas in the northeasterly part of the domain. This land-use type is characterized by a relatively open landscape with a roughness length between 3 and 10 cm. Due to the relatively low and gentle hills the wind speed distribution at 50 m height is dominated by surface roughness and displacement height rather than orography. These effects have been separated by three test runs with an identical rough-

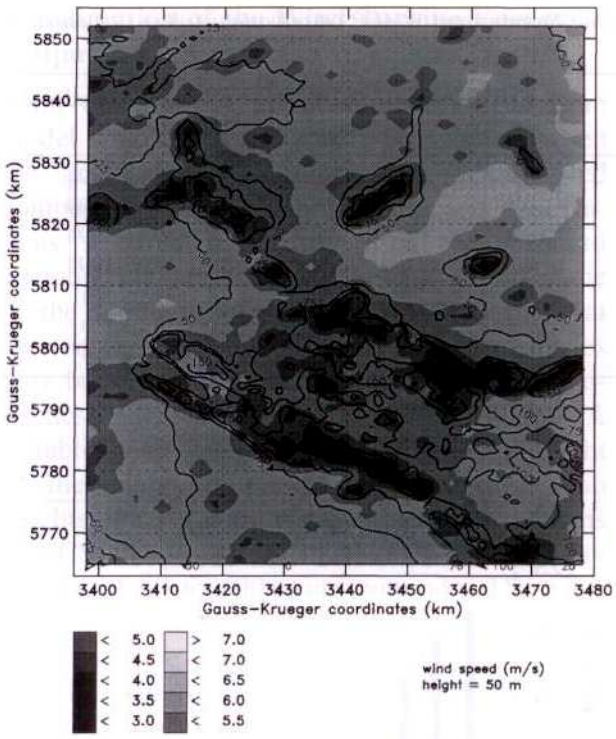

Fig. 6. Regional distribution of the weighted mean wind speed at 50 m height above ground. The orography contour lines are included for orientation

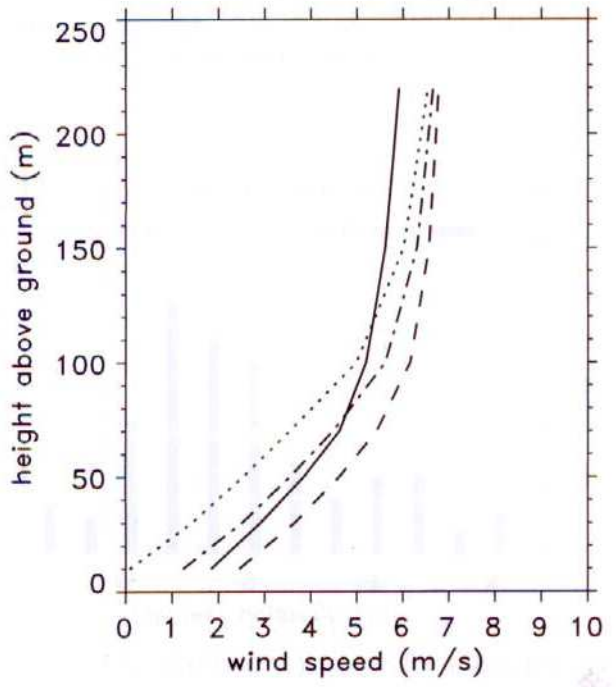

Fig. 7. Vertical profiles of wind speed over flat smooth terrain (solid line) and a forested hilly site (dashed line: same roughness length at both locations and no displacement height, dash-dotted line: different roughness length but no displacement height; dotted line: different roughness length and displacement height over the forested hill)

ness length over the whole simulation domain (run 1), applying realistic roughness length values but no displacement height for the forested regions (run 2) and accounting for the displacement height in addition to the realistic roughness distribution (run 3). We compare the vertical wind speed profiles for these three test cases for a location over a forested hill (coordinates 3434/5787) with the reference profile over farmland in flat terrain (coordinates 3411/5782). For run 1 the orographically induced acceleration shifts the whole profile to higher values. For run 2 the roughness effect at the hilly site dominates the orographically induced acceleration below 70 m height. Above this height the wind profile approaches that of the case 1 profile. With the displacement height included a further wind speed reduction occurs and the orography effect becomes evident above 100 m height (Fig. 7).

4.2 Verification with Measurements

There were 4 weather stations belonging to the German Weather Service (DWD) and 3 WMEP stations (a special German Wind Measuring and Evaluation Program for wind energy assessment) inside the simulation domain. Their locations are indicated in Fig. 4 and the coordinates are given in Table 1. The time period of the data from the 4 synoptic stations (1980–1994) is nearly identical with the time frame of the radiaosonde data used as forcing (1979–1991). The WMEP stations were only operated for 35 months during 1991 to 1993. All data were measured at 10 m height over farmland or an airport area (Greven) except for wind speed at the station Osnabrück. Here, the measurement height of 18 m indicates the existence of some obstacles close to the anemometer. We have extrapolated the wind speed frequency distribution down to 10 m by use of a simple power law.

The simulated data are the weighted averages of all cluster simulations and represent the volume average of the respective grid cell. Despite the fact that we compare point measurements with volume averages over a 1×1 km grid box the simulations agree well with the DWD-data while their differences to the WMEP stations are larger. The much shorter time period of the WMEP measurements and to some extent the

Table 1. *Mean Wind Speed u and Energy Flux Density $\bar{E}$ at Weather Stations and WMEP Observations (obs.) Compared to Simulated Data (sim.). The Coordinates refer to Fig. 4*

Station	Coordinates x/y	$u(m/s)$ obs.	u (m/s) sim.	$\bar{E}(W/m^2)$ obs.	$\bar{E}(W/m^2)$ sim.	obs. period
Diepholz	3455/5828	3.8	3.6	89	70	1980–1994
Hopsten	3401/5801	4.1	4.1	99	100	1980–1994
Greven	3410/5778	3.7	3.6	74	76	1980–1994
Osnabr.	3435/5791	3.2	3.0	42	63	1980–1994
WMEP 1	3452/5831	3.5	4.0	70	100	34 month
WMEP 2	3436/5828	3.4	3.6	74	75	35 month
WMEP 3	3458/5809	2.9	3.5	45	75	35 month

sheltering effects of bushes or trees close to the measuring sites may have been the reason for this.

In terms of available wind power potential, the mean of the energy flux density $\bar{E}[W/m^2]$ is the variable of interest rather than the wind speed because of the non-linear relationship:

$$\bar{E} = \sum_{i=1}^{n} \frac{1}{2} \rho \left[v_{x_i}^2 + v_{y_i}^2 + v_{z_i}^2 \right]^{\frac{3}{2}} \cdot f_i \qquad (1)$$

$\rho[kg/m^3]$ is the air density and $v_{x,y,z}[m/s]$ denotes the wind speed components, f_i is the frequency of occurrence of cluster i. In our case n equals 143. The numbers in Table 1. represent the weighted mean $\bar{E}$ of the energy flux density E_i for each cluster i. For the DWD and WMEP stations $\bar{E}$ was calculated from the frequency distribution of wind speed given in 1 m/s intervals. The largest difference between the DWD stations and the simulated values is for the station Osnabrück where the surroundings are not representative of the respective grid box. The smaller $\bar{E}$ values for the WMEP stations compared to the simulations are not necessarily caused by the different time period. An inspection of the corresponding yearly means at the DWD stations showed no clear trend on a deviation compared to the long-term mean.

The frequency distribution for wind speed and -direction was derived from the cluster data by grouping the wind speed into 1 m/s classes and the wind direction into 12 sectors and summing the corresponding cluster frequency for each group. Figure 8 shows the simulated and measured frequency distributions for the grid cell 'Greven'. The general features show larger differences at low wind speeds and an over-representation of southwesterly wind directions by the simulations, and these are typical for all 7 measurement stations.

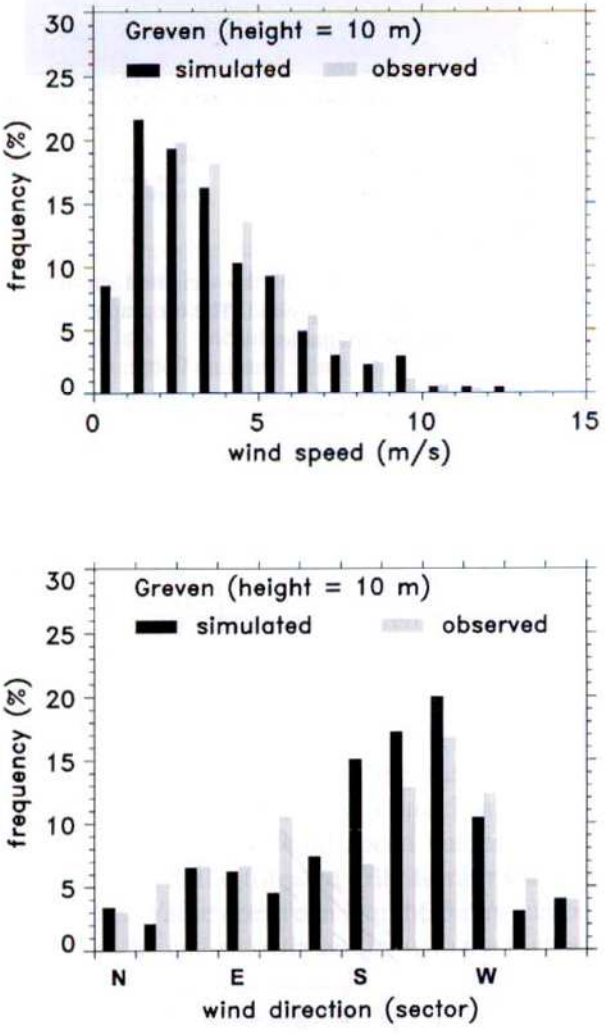

Fig. 8. Frequency distribution of wind speed and direction for the observation station Greven

5. Estimation of the Wind Turbine Energy Output

Point observations and volume averages from model simulations are hardly comparable when the spatial scales do not match. Wind speed comparisons between model data and observations at greater heights (than the standard anemometer height) could help to avoid some of the problems of scale mismatch because at greater height disturbances by close obstacles may be less important. The area of representativeness increases with increasing height. A suitable measure for wind field verification might be the energy output of wind turbines. Hub heights of early wind energy conversion systems (WECS) ranged from 30 to 50 m while today heights of 60 to 100 m are common. The rotor diameter meanwhile reaches more than 60 m. WECS can be considered as measuring devices for the kinetic energy content of the air integrating over an air volume, depending in size on the geometrical dimensions of the turbine. In any case, the area of representativeness is much larger than that of a near-surface anemometer.

The mean electrical energy output $\overline{EP}[Ws]$ of a wind turbine over a particular time period $T[s]$ is given by

$$\overline{EP} = \frac{1}{2}\rho A \int_0^T c_p(u) u^3 dt \tag{2}$$

With the power coefficient c_p (electrical power/available wind power)

$$c_p(u) = \frac{P(u)}{1/2\rho A\, u^3} \tag{3}$$

we can write

$$\overline{EP} = \int_0^\infty P(u) f(u) du \cdot T \tag{4}$$

where $f(u)$ represents the frequency distribution of wind speed $u[m/s]$ during the time period T [s] (Mengelkamp, 1988). The power curve $P(u)$ [W] describes the dependence of the electrical power output on wind speed. It is a characteristic of a wind turbine and usually provided by the manufacturer. A $[m^2]$ is the rotor swept area and ρ the air density.

The stars in Fig. 4 indicate locations of 46 wind turbines the output of which is documented

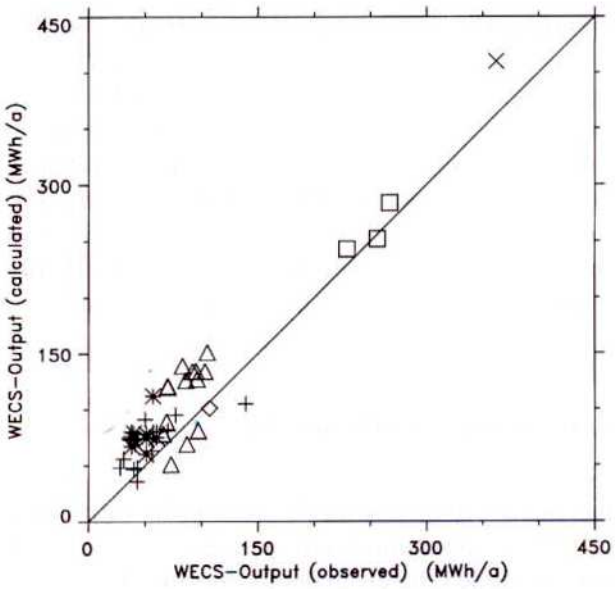

Fig. 9. Actual and calculated mean electrical energy output of wind turbines. Different symbols refer to different types of wind turbines characterized by their rated power (plus sign: 50 kW rated power, asterix: 75 kW, triangle: 80 kW, diamond: 100 kW, square: 150 kW and cross: 300 kW)

in a WMEP statistic. Only smaller WECS are considered with hub heights ranging from 25 to 41 m and a rated power between 50 and 300 kW. The operation time period ranges from 1 to 5 years. $f(u)$ was calculated for the grid cells corresponding to the locations of the turbines. The calculated mean yearly electrical energy production is compared to the actual wind turbine output (Fig. 9). Larger differences of up to 100 percent, can be found particularly for the smaller WECS. Because the wind power, which is the kinetic energy of an air volume passing the rotor swept area of a wind turbine in a certain time, is a cubic function of wind speed relative uncertainties in wind power, and consequently in the electrical energy output of wind turbines, are much larger than in wind speed. With complex orography and roughness conditions the difference in scale between a model grid and the area of influence for a wind turbine is particularly evident for smaller WECS. The interpolation of orography on the model grid might be of major importance. Also the different time periods for the wind simulations and the WECS operation may be a major source of the deviation. Small-scale temporal variations in the wind field are not considered in the cluster analysis but may

significantly control the WECS energy output. Uncertainties in the power curve determination may also add some error to the calculated output. Despite these facts it is obvious that there is no bias or systematic trend of deviation between calculated and actual WECS energy output. The increasing size of wind turbines and their increased energy production will drastically reduce the relative deviation of the calculated from the actual output.

6. Conclusion and Outlook

The statistical-dynamical downscaling approach has proven to be a suitable tool for the estimation of a high-resolution climatological wind field over complex heterogeneous terrain. 143 reference states used to describe the climatological forcing statistics were estimated by a cluster analysis based on 12-years time series of radiosonde data. We have highlighted the advantages compared to a fixed classification scheme but without prove which would require an additional similar computational effort.

Use of a non-hydrostatic mesoscale model permitted a spatial resolution of 1×1 km which made feasable a comparison with observations. The deviation of simulated and measured mean wind speed was below 0.2 m/s for the long term means at the synoptic stations but larger for the shorter records at WMEP stations. Differences of up to 30 percent were found for the energy flux density which, however, is more sensitive than the mean wind speed to any uncertainties in the downscaling procedure due to its dependence on wind speed cubed. Larger differences for very low wind speed values and an over-representation of southwesterly directions were apparent in the respective frequency distributions.

By combining wind speed frequency distributions and power curves of wind turbines we have calculated the mean yearly electricity production. Relative differences of up to 100 percent compared to the actual data were found for the smallest turbines but no bias and systematic trend of a deviation was obvious. We had access to the WMEP statistics only for the early small wind turbines. With increasing wind turbine size we expect a dramatic reduction in the relative differences.

Bearing in mind the 3rd power dependency on wind speed, wind turbine energy output becomes a reliable measure for verifying simulated climatological wind fields. The advantages of wind turbines compared to standard anemometers are obvious. Due to their greater height and larger rotor area disturbances by close obstacles become less important and their energy production is representative for a much larger air volume which might come close to the resolution which can today be achieved with non-hydrostatic mesoscale models.

This study has also proven that an estimation of the mean energy output of planned wind turbines might be possible without near-surface measurements with reasonable accuracy, certainly enough for modern large wind turbines, even over complex terrain.

Acknowledgement

The radiosonde data were purchased from the German Weather service. Thanks go in particular to U. Pflüger (German Weather Service, Offenbach) for performing the cluster analysis. Discussions with H. Kapitza and A. Rhodin (GKSS Forschungszentrum, Geesthacht) on the model GESIMA are much appreciated. ISET (Institute for Solar Energy Technique, Kassel) kindly provided the meteorological data of the WMEP stations and the WECS output data. This study was partly sponsored by the Deutsche Bundesstiftung Umwelt, Osnabrück.

References

Anderson, D. A., Tannehill, J. C., Pletcher, R. H., 1984: *Computational Fluid Mechanics and Heat Transfer.* New York: Hemisphere Publishing Corporation, pp. 599.

Bergström, H., 1996: A climatological study of boundary layer wind speed using a meso-scale higher-order closure model. *J. Appl. Meteor.*, **35**, 1291–1306.

Bhumralkar, C. M., Mancuso, R. L., Ludwig, F. L., Renne, D. S., 1980: A practical and economic method for estimating wind characteristics at potential wind energy conversion sites. *Solar Energy*, **25**, 55–65.

Bougeault, P., Lacarrere, P., 1989: Parameterization of orography-induced turbulence in a mesobeta-scale model. *Mon. Wea. Rev.*, **117**, 1870–1888.

Brücher, W., Kerschgens, M. J., Steffany, F., 1994: On the generation of synthetic wind roses in orographically structured terrain. *Theor. Appl. Climatol.*, **48**, 203–207.

Dittmann, E., Thehos, R., Pflüger, U., Baldrusch, M., Büchen, M., 1995: Comparison of dispersion calculations between TA-Luft and a method based on a more complex model combination (FITNAH/LBDM). *Int. J. Environment and Pollution*, **5**(4–6), 748–757.

Endlich, R. M., Ludwig, F. L., Bhumralkar, C. M., Estoque, M. A., 1982: A diagnostic model for estimating winds at potential sites for wind turbines. *J. Appl. Meteor.*, **21**, 1441–1454.

Eppel, D., Kapitza, H., Claussen, M., Jacob, D., Koch, W., Levkov, L., Mengelkamp, H.-T., Werrmann, N., 1995: The non-hydrostatic mesoscale model GESIMA. Part II. parameterizations and applications. *Beitr. Phys. Atmos.*, **68**, (1), 15–41.

Frey-Buness, F., Heimann, D., Sausen, R., 1995: A statistical-dynamical downscaling procedure for global climate simulations. *Theor. Appl. Climatol.*, **50**, 117–131.

Giorgi, F., Mearns, L. O., 1991: Approaches to the simulation of regional climate change: a review. *Rev. Geophys.*, **29**(2), 191–216.

Groß, G., 1996: On the applicability of numerical mass-consistent wind field models. *Bound.-Layer Meteor.*, **77**, 379–394.

Guo, X., Palutikof, J. P., 1990: A study of two mass-consistent models: problems and possible solutions. *Bound.-Layer Meteor.*, **53**, 303–332.

Heimann, D., 1986: Estimation of regional surface layer wind field characteristics using a three-layer mesoscale model. *Beitr. Phys. Atmos.*, **59**(4), 518–537.

Kalkstein, L. S., Tan, G., Skindlov, J. A., 1987: An evaluation of three clustering procedures for use in synoptic climatological classification. *J. Climate Appl. Meteorol.*, **26**, 717–730.

Kapitza, H., Eppel, D., 1992: The non-hydrostatic mesoscale model GESIMA. Part I: dynamical equations and tests. *Beitr. Phys. Atmos.*, **65**(2), 129–146.

Lalas, D. P., Ratto, C. F., (ed.), 1996: *Modelling of Atmospheric Flow Fields*. Singapore: World Scientific Publishing, pp. 753.

Mellor, G. L., Yamada, T., 1974: A hierarchy of turbulence closure models for planetary boundary layers. *J. Atmos. Sci.*, **31**, 1791–1806.

Mengelkamp, H.-T., 1988: On the energy output estimation of wind turbines. *Int. J. Energy Res.*, **12**, 113–123.

Mengelkamp, H.-T., 1991: Boundary-layer structure over an inhomogeneous surface: simulation with a non-hydrostatic mesoscale model. *Bound.-Layer Meteor.*, **57**, 323–341.

Sandström, S., 1997: Simulations of the climatological wind field in the Baltic Sea area using a mesoscale higher-order closure model. *J. Appl. Meteor.*, **36**, 1541–1552.

Segal, M., Mahrer, Y., Pielke, R., 1982: Numerical study of wind energy characteristics over heterogeneous terrain – central Israel case study. *Bound.-Layer Meteor.*, **22**, 373–392.

Sherman, C. A., 1978: A mass-consistent model for wind-fields over complex terrain. *J. Appl. Meteor.*, **17**, 312–319.

Storch, H., von 1995: Inconsistencies at the interface of climate impact studies and global climate research. *Meteorol. Zeitschrift, N. F.*, **4**, 72–80.

Troen, I., Petersen, E. L., 1989: *European Wind Atlas*. Riso National Laboratory, Roskilde, pp. 656. ISBN 87-550-1482-8.

Wieringa, J., 1983: Description requirements for assessment of non-ideal wind stations – for example Aachen. *J. Wind Engineering and Industrial Aerodynamics*, **11**, 121–131.

Wieringa, J., 1986: Roughness-dependent geographical interpolation of surface wind speed averages. *Quart. J. Roy. Meteor. Soc.*, **112**, 867–889.

Wippermann, F., Groß, G., 1981: On the construction of orographically influenced wind roses for given distributions of the large-scale wind. *Beitr. Phys. Atmos.*, **54**, 492–501.

Author's address: H.-T. Mengelkamp, Institute for Atmospheric Physics, GKSS-Forschungszentrum, D-21502 Geesthacht, Germany.